# Comparative Study of Two Phase Locked Loop Algorithms for Grid-Connected Inverter Synchronization

[1]M. H. Ali,  [1]*A. A. Sisa and [2]A. B. Ahmed

[1]Department of Physics, Bayero University Kano, Kano, Nigeria
[2]Department of Physics, Gombe State University. PMB 127 Gombe, Nigeria

Corresponding Author: sisa@gsu.edu.ng

## ABSTRACT

This paper assesses the Phase-Locked Loop (PLL) algorithm's performance in synchronizing Grid-Connected Inverters with the utility grid. Although two primary synchronization techniques, namely *αβPLL* and *dq*PLLs, are commonly used, specific conditions suitable for each technique have not been thoroughly documented. The evaluation process involves both theoretical testing and simulation in the MATLAB/Simulink environment. The results demonstrate that the *αβ*PLL technique exhibits robust performance, achieving precise grid voltage synchronization under both normal and abnormal grid conditions. Furthermore, it demonstrates effective harmonic filtering capabilities, achieving a Total Harmonic Distortion (THD) of 1.71% and 1.73% when the grid voltage is distorted with harmonics. Importantly, these THD results for the *αβ*PLL technique adhere to the IEEE Standard 929-2000's specified limits. In contrast, the *dq*PLL technique does not perform effectively, particularly under abnormal grid conditions. It struggles with synchronization and harmonic filtering, resulting in THD values that exceed the specified limits. The findings indicate that *αβ*PLL synchronization is a promising technique, capable of facilitating successful grid-inverter power synchronization even in adverse grid conditions. This proficiency in grid integration enhances the potential for injecting more renewable energy into the grid, contributing to increased power availability for distribution to households.

**Keywords:** Distributed Power Generation, Synchronization, Grid-Connected inverter, Phase Locked Loop, Matlab/Simulink and Model-Based Design,

## INTRODUCTION

Fossil base fuel for generation of power impose problem in the environment which include greenhouse effect and global warming (Suleiman et al., 2016). This result in the increasing installation of distributed power generation based on renewable energy sources (RES) to minimize these environmental hazards. The use of this form of energy generation has become trendy to enhance the stability and reliability of the utility grid (Ali et al., 2022). Among the various RES solar photovoltaic systems (PVS) is more prioritized.

The integration of the solar PVS with the utility grid causes controllability complication due to the interaction of several grid-connected inverters (GCIs) tied to the utility grid at the point of common coupling (PCC) (Ali et al., 2022; Xu et al., 2019). For this purposeful interaction, there is need for synchronization of utility grid parameters with that of the GCIs (Yu et al., 2022). A number of synchronization technique for GCI were reported and categorised into frequency-domain (e.g. discrete Fourier transform and recursive discrete Fourier transform) and time-domain (e.g. Zero crossing detection and phase locked loop) synchronizations techniques (Jaalam et al., 2016). It is not an exaggeration to state that the phase locked loop (PLL) is the first choice for synchronization of GCIs to the utility grid due to its simplicity of stability analysis.

The stationary reference frame PLL (*αβ PLL*) and synchronous reference frame (*dqPLL* ) are the most widely used single phase PLL

(Xu et al., 2019). The basic notion behind them is creating a fictitious quadrature signal for transferring information into the *αβ*-frame and *dq*- frame. Because there is no physical rotational frequency of the GCI with the utility grid impedance, the PLL relies only on phase detection to acquire and maintain synchronization; hence, the utility grid is prone to disturbance and transients. (Akhtar & Saha, 2020). Information about the utility grid fundamental voltage component, such as the instantaneous phase, frequency and amplitude, for tracking its phase and frequency is vital for synchronization (L. Hadjidemetriou et al., 2016). As such an ideal PLL must competently track these information in order to eliminate the disturbances and harmonics under various grid conditions (Hadjidemetriou et al., 2019). However, the conditions suitable for each of these two techniques are not yet reported.

In literature, several studies have been carried out to address the gap in technical challenges of synchronizing GCI with the utility grid. Most of the recent research focus on rejection of disturbances like phase deviation, frequency deviation and harmonics in the grid by the GCI, inspired by the works of (Yu et al., 2022; Meral & Celik, 2018; Rey-boue, 2017; Sepahvand et al., 2021; Youness et al., 2019) and stability in faulty and weak grid by (De la Sen, 2007; Wang et al., 2019; Zhang et al., 2015). In this work, comparative study of the performance of single-phase *αβPLL* and *dqPLL* for synchronizing GCI with utility grid under adverse grid conditions was carried out. To verify the effectiveness of these techniques, stability analysis was performed based on Routh-Hurwitz test.

## MATHEMATICAL FORMULATIONS

Phase detector (PD), loop filter (LF), and voltage control oscillator (VCO) are the three fundamental building blocks that make up the basic configuration of a Phase Locked Loop (PLL) with transport delay (TD) based on an in-quadrature signal generator (In-QSG) phase detector, which is depicted in Figure 1 (Akhtar & Saha, 2020). The phase difference information between the input signal and the PLL output is provided by PD, which is routed via a loop filter (LF) with low-pass filtering characteristics to reduce the phase error between the input grid signal and the PLL output to zero. The VCO creates a phase signal depending on the LF signal. As illustrated in Figure 1, PD in the PLL model consists of TD based on In-QSG followed by Transformation Matrix. The importance of In-QSG-based TD in attaining synchronization is assessed using phasor and frequency domain analysis.
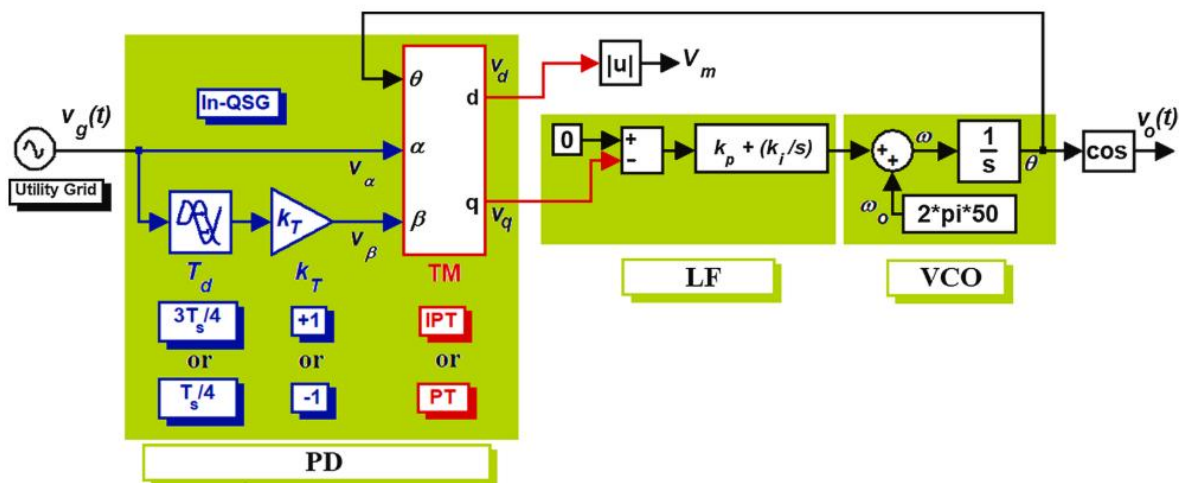


**Figure 1:** Theoretical model of Phase Locked Loop (PLL) with TD based on In-QSG phase detector(Akhtar & Saha, 2020)

**Phasor Analysis**

Consider the grid voltage signal, $v_g(t)$, delivered to In-QSG as a single signal in the stationary reference frame depicted in Figure 1.

$$v_g(t) = v_\alpha(t) = V_m \sin(\Psi_g) = V_m \sin(\omega_g t + \phi) \tag{1}$$

where Vm is the grid voltage amplitude, $\phi$ is the grid voltage phase, and $\omega_g$ is the grid angular frequency. eqn. (1) represents the initial phase displacement at which grid voltage is measured. If we add a time delay $T_d$ and gain $K_T$ to eqn. (1), we get another signal in the $v_\beta(t)$ .

$$v_\beta(t) = K_T v_g(t - T_d) = K_T V_m \sin[\omega_g(t - T_d) - \phi] \tag{2}$$

The signal $v_\alpha(t)$ is orthogonal to $v_\beta(t)$ if the phase difference between them is 270° or 90°, which corresponds to $T_d$ as $3T_s/4$ and $T_s/4$ respectively. If the rotation direction of the grid angular frequency $\omega_g$, is counter clockwise, the phasor forms of equations (1) and (2) are $V_\alpha$ and $V_\beta$, respectively.

$$V_\alpha = V_m \langle -\phi$$
$$V_\beta = V_m \langle -\phi \pm 90° \tag{3}$$

The signal $v_\beta(t)$ either lags or leads from $v_\alpha(t)$ by 90° under different values of $T_d$ and $K_T$.

**Transformation Matrix of the Model**

Clarke and Park transformations are used in high performance architecture in single-phase power system analysis. Current and voltage are represented in term of space vector which is in either stationary αβ reference frame or synchronous dq reference frame. Orthogonal signals in αβ- reference frame and dq-reference frame are transformed into a rotating reference frame and stationary reference frame respectively using the theorem for phase detector operation i.e. eqn. (4) and (5). Transformation matrix (TM) of Park and Clarke's are given in. (6) and (7) respectively (Hadjidemetriou et al., 2016).

$$V_{dq}(t) = \begin{bmatrix} \cos\Psi_e & \sin\Psi_e \\ -\sin\Psi_e & \cos\Psi_e \end{bmatrix} V_{\alpha\beta}(t) \tag{4}$$

$$V_{\alpha\beta}(t) = \begin{bmatrix} \cos\Psi_e & -\sin\Psi_e \\ \sin\Psi_e & \cos\Psi_e \end{bmatrix} V_{dq}(t) \tag{5}$$

$$T_{dq} = \begin{bmatrix} \cos\Psi_e & \sin\Psi_e \\ -\sin\Psi_e & \cos\Psi_e \end{bmatrix} \tag{6}$$

$$T_{\alpha\beta} = \begin{bmatrix} \cos\Psi_e & -\sin\Psi_e \\ \sin\Psi_e & \cos\Psi_e \end{bmatrix} \tag{7}$$

**Frequency Domain Analysis**

The frequency response of the reference signal from the grid is used to measure the influence of grid disturbances such as grid phase angle variation, frequency deviation, and harmonic distortions. The transfer function of the model in Figure 2 may be determined by taking the Laplace transform of eqns. (1) and (2). The transfer function of the models uses a ratio of polynomials to explain the relationship between the inputs and outputs of a system. The order of the model is the same as the order of the denominator polynomial. The denominator polynomial roots are referred to as the model poles. The numerator polynomial roots are referred to as the model zeros. A Transfer function model's parameters include its poles, zeros, and transport delays. In continuous time, a Transfer function model has the form:

$$Y(s) = \frac{Num(s)}{Den(s)} U(s) + E(s) \qquad\qquad (8)$$

where, Y(s), U(s) and E(s) represent the Laplace transforms of the output, input and noise, respectively. Num(s) and Den(s) represent the numerator and denominator polynomials that define the relationship between the input and the output.

**Routh-Hurwitz Stability Criteria**

To assess the system's stability, we must discover the roots of the characteristic equation, often known as poles. The characteristic equations in the analysis are typically big and complicated. As a result,

simplifying them into roots is challenging. In such cases, the Routh-Hurwitz Method provides a straightforward and rapid way to evaluate stability without having to decompose the characteristic equation (De la Sen, 2007).

The Routh Hurwitz Stability Criterion is based on the characteristic equation coefficients being ordered into an array, commonly known as the Routh Array. Assume the characteristic equation of a control system is as follows:

$$q(s) = a_o S^n + a_1 S^{n-1} + a_2 S^{n-2} + \dots\dots + a_{n-1}S + a_n = 0 \qquad (9)$$

Now, from the given equation, we will form Routh Array as shown in figure 2 below:



**Figure 2:** Routh Array

The coefficients $a_o$, $a_1$ ... $a_n$ are extracted from the equation and organized as illustrated. These elements are used to compute other elements. For a system to be stable, each term in the first column of the Routh Array generated by its characteristic equation must be positive if $a_o>0$. If this condition is not satisfied, the system is unstable, and the number of sign changes in the first column of the Routh Array corresponds to the number of roots of the characteristic equation in the right half of the s-plane.

## METHOD

The performance of $\alpha\beta$PLL *and dqPLL* algorithm were evaluated based on three adverse grid condition. The conditions were:

1. Phase jump: When a phase jump of 40° is subjected to the grid voltage.

2. Frequency shift: When a frequency shift of $\pm 1$ Hz is subjected to the grid voltage.

3. Harmonics: When harmonic of 2nd and 3rd order are subjected to the grid voltage. In addition, the stability analysis of the PLLs algorithm was also conducted. We carried out this comparative study through simulation using Model-Based Design in MATLAB/SIMULINK 2016b platform. The synchronization techniques were as well tested and validated using the SIM POWER SYSTEM TOOLBOX of the platform under the above grid conditions. Also, analysis of stability of the techniques was conducted using the SYSTEM IDENTIFICATION TOOLBOX of the Platform. The Phase Locked Loop algorithm for synchronizing PV fed Voltage Source Inverter (GCI), were test with a model of 2000VA inverter
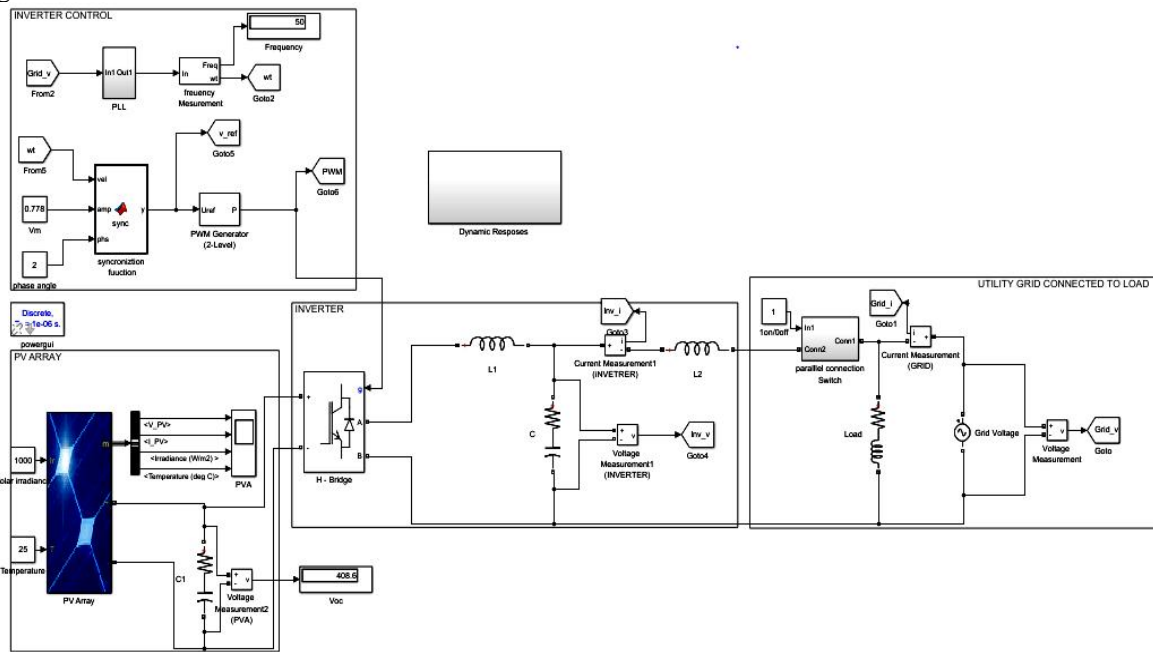
integrated with the utility grid as shown in Figure 2.



**Figure 3:** model based design of the Grid-connected PV system

Figure 4 (a) and (b) depicts the model-based design of a stationary *αβ* reference frame and synchronous *dq* reference frame Phase Locked Loop (PLL). The model was created using the Simulink environment for multi domain simulation and Model-Based Design and was based on equations (1) through (9). It enables embedded system level design, simulation, automatic code creation, and continuous testing and verification. Simulink's modeling and simulation tools include a graphical editor, customisable block libraries (Simpower Blocksets), and solvers. It is MATLAB integrated, which enable us to insert MATLAB algorithms into models and export simulation results to the MATLAB workspace for further analysis using Data Logging.
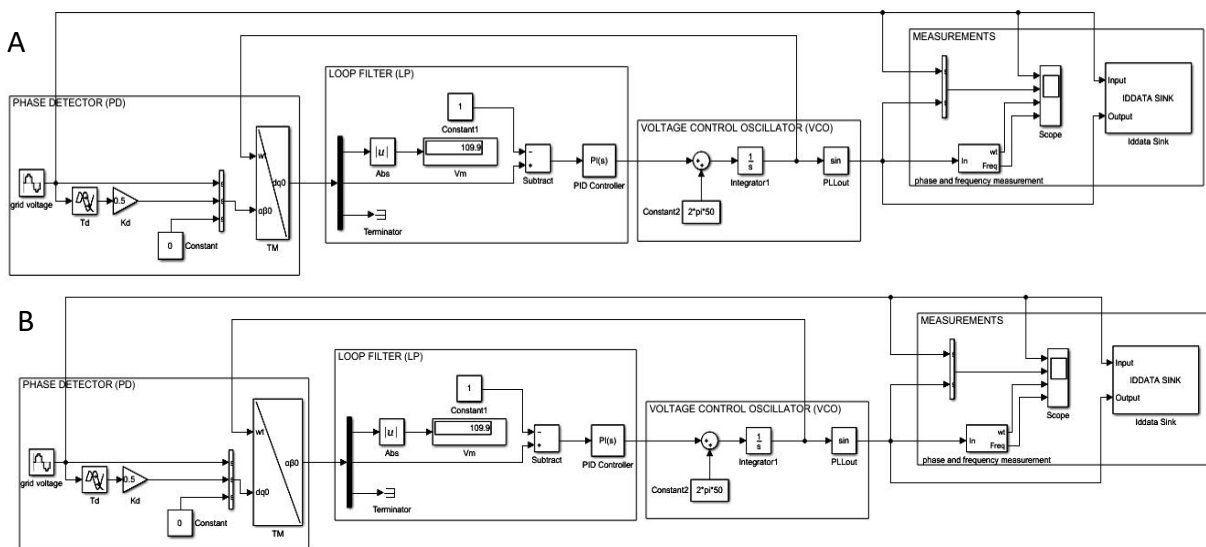


**Figure 4:** The model based design of grid connected PV System (a) Stationary αβ reference frame PLL (b) synchronous dq reference frame PLL

## RESULTS AND DISCUSSION

The response performance of dynamic state of Integrated Model of the PV fed GCI for the Stationary αβ reference frame Phase Locked Loop (PLL) and the Synchronous dq reference Phase Locked Loop (PLL) algorithm under the test conditions were presented as follows.

**Responses of the αβPLL and dqPLL algorithms when Phase jump is subjected to the grid voltage.**

The synchronization responses of the integrated model of the PV fed GCI for the αβPLL and dqPLL when subjected to phase jump of 40º the grid voltage are shown in Figure 5 to 8.
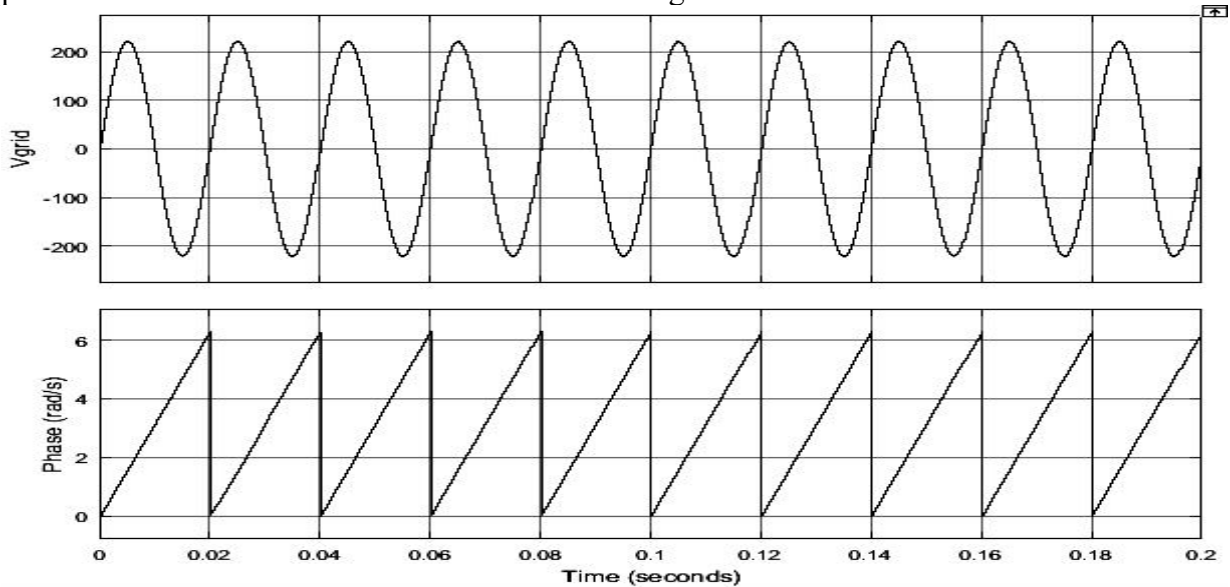


**Figure 5:** Grid voltage waveform and phase angle detected by the αβPLL
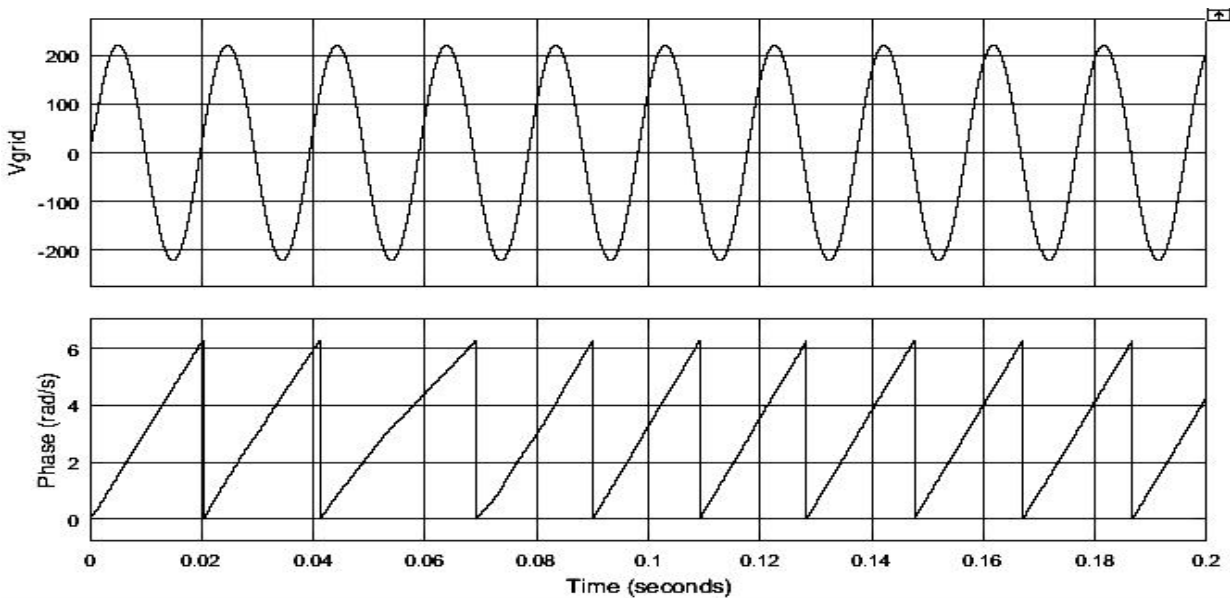


**Figure 6:** Grid voltage waveform and phase angle detected by the dqPLL
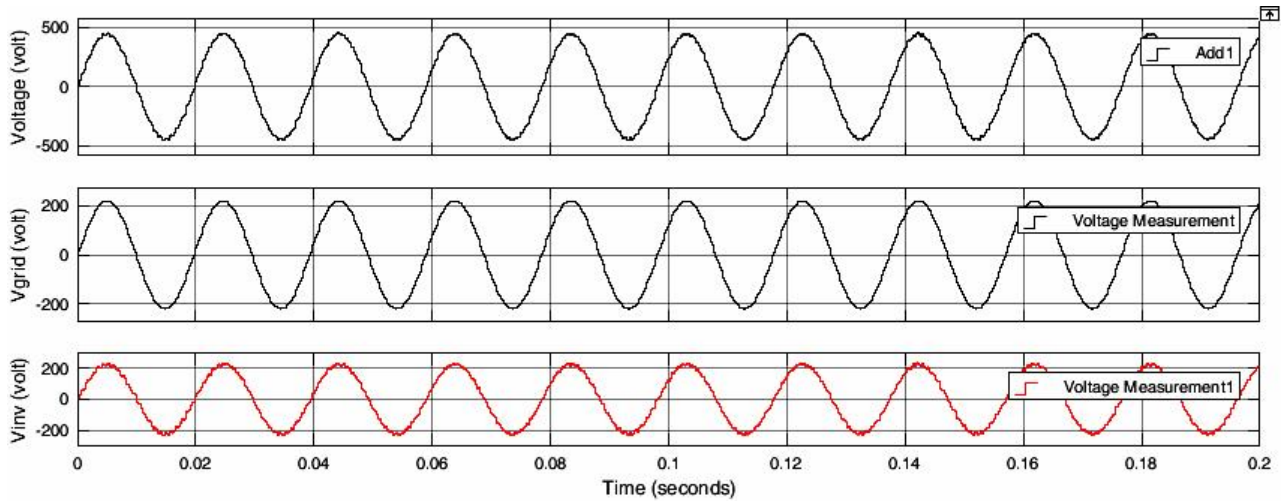
**Figure 7:** Synchronised grid and inverter voltages when GCI is integrated with the αβPLL
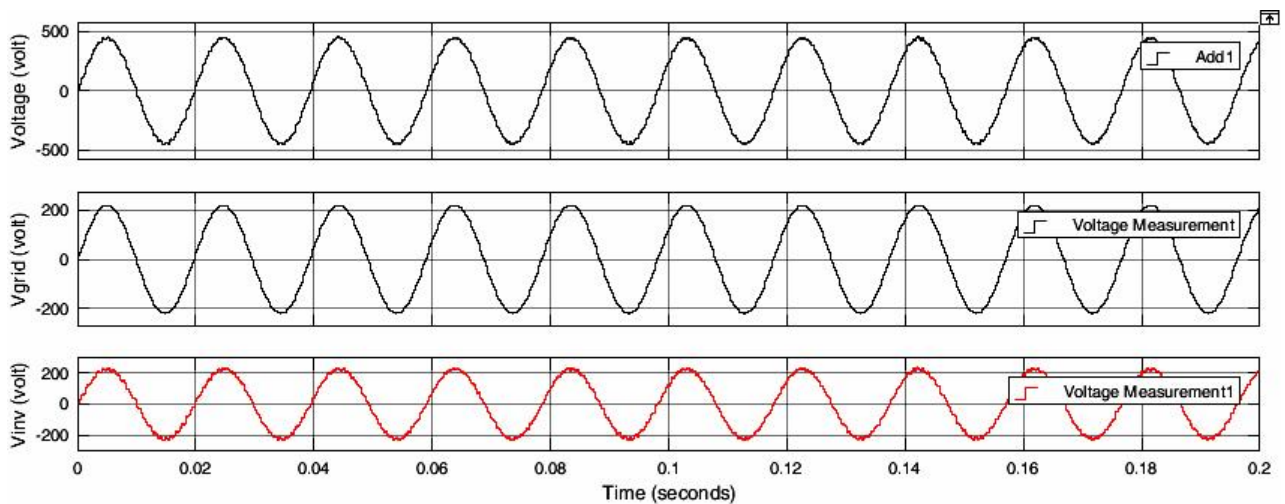


**Figure 8:** Synchronised grid and inverter voltages when GCI is integrated with the dqPLL

From Figure 5, it can be seen that the detected phase which is the time integral of the angular frequency is perfectly triangular for αβPLL while for dqPLL is not perfectly triangular as depicted in Figure 6. The good phase detection of the αβPLL result in an estimated grid voltage having an imperceptible variation, this results in obtaining a perfectly periodic reference signal which was used to generate pulses to drive the gate of the inverter. From Figure 7, time for orthogonal signal setup for αβPLL was found to be 15ms with an initial synchronization time of 20ms, while for dqPLL, time for orthogonal signal setup was found to be 25ms with an initial synchronization time of 30ms. The αβPLL have better orthogonal signal setup and initial synchronization time compared to dqPLL. This result in perfectly synchronizing grid and the inverter voltage by the αβPLL algorithm from the start of simulation as shown in Figure 7.

**Responses of the αβPLL and dqPLL algorithms when Frequency shift is subjected to the grid voltage.**

The synchronization responses of the integrated model of the PV fed GCI for the αβPLL and dqPLL when subjected to Frequency shift of 1 Hz is shown in Figures 9 to 12 for both merged and synchronized grid and inverter voltage.

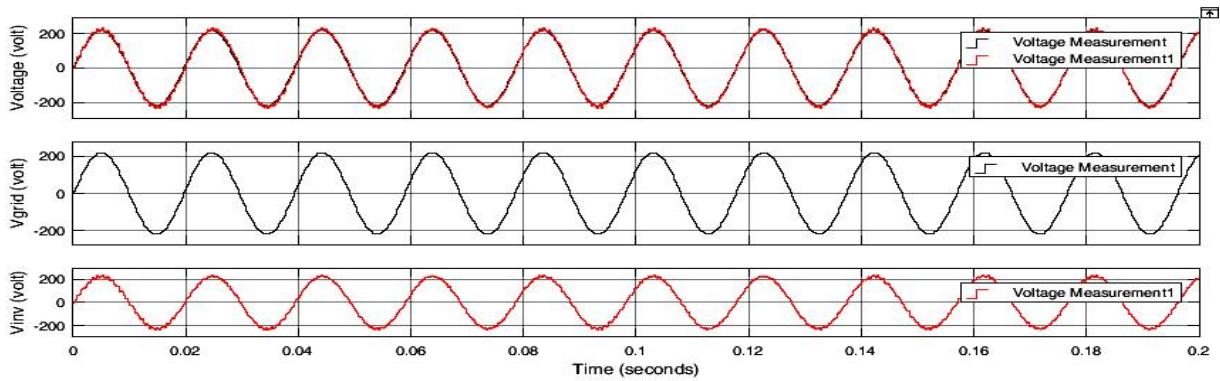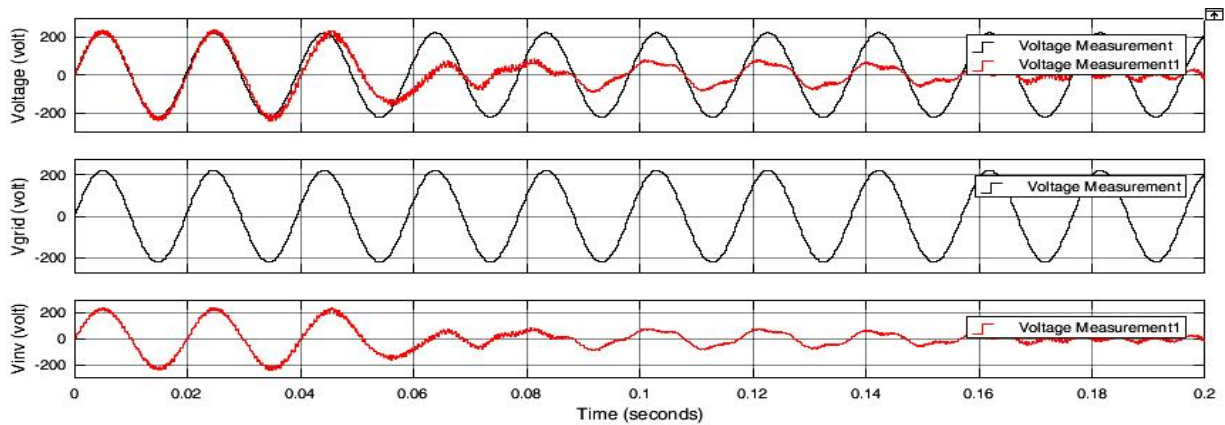**Figure 9:** Merged grid and inverter voltages when GCI is integrated with the αβPLL



**Figure 10:** Merged grid and inverter voltages when GCI is integrated with the dqPL



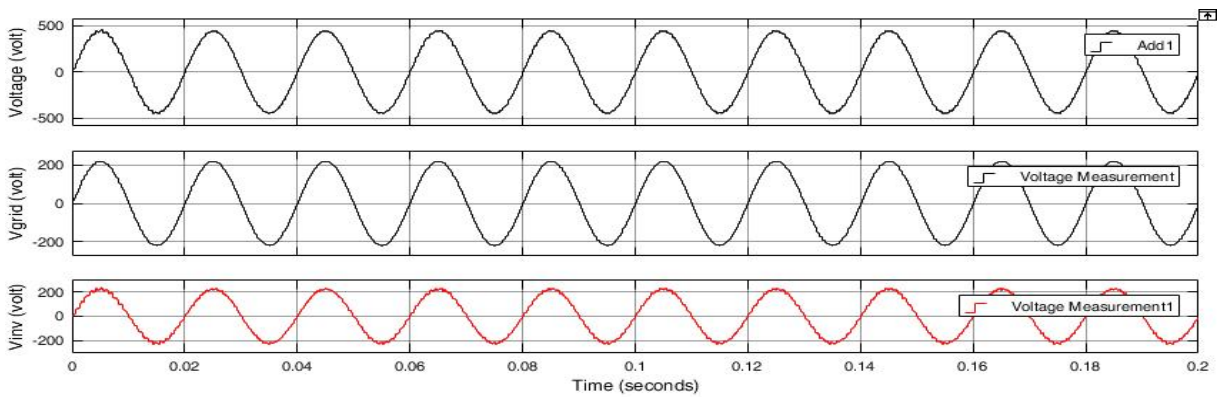**Figure 11:** Synchronised grid and inverter voltages when GCI is integrated with the αβPLL
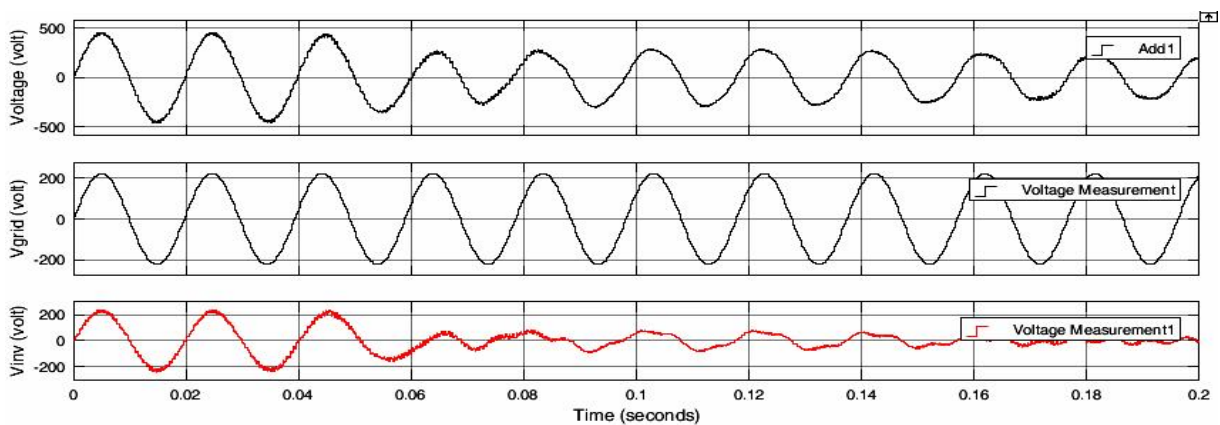


**Figure 12:** Synchronised grid and inverter voltages when GCI is integrated with the dqPLL

It was observed that time for orthogonal signal setup for αβPLL to be 15ms with an initial synchronization time of 20ms, while time for orthogonal signal setup was found to be 25ms and grid-inverter voltages synchronization was lost around 60ms for dqPLL as shown in Figure 10 and 12. The good orthogonal signal setup and initial synchronization time of the αβPLL result in perfectly synchronizing grid and the inverter voltage from the start of simulation as depicted in Figure 9 and 11.

**Responses of the αβPLL and dqPLL algorithms when Harmonic distortion is subjected to the grid voltage.**

The simulation data of the grid and inverter voltage were export to the MATLAB workspace using data logging. Harmonics analysis was conducted when the grid voltage is subjected to $2^{nd}$ and $3^{rd}$ order harmonics and the result in Figure 13 to 16 were obtained.
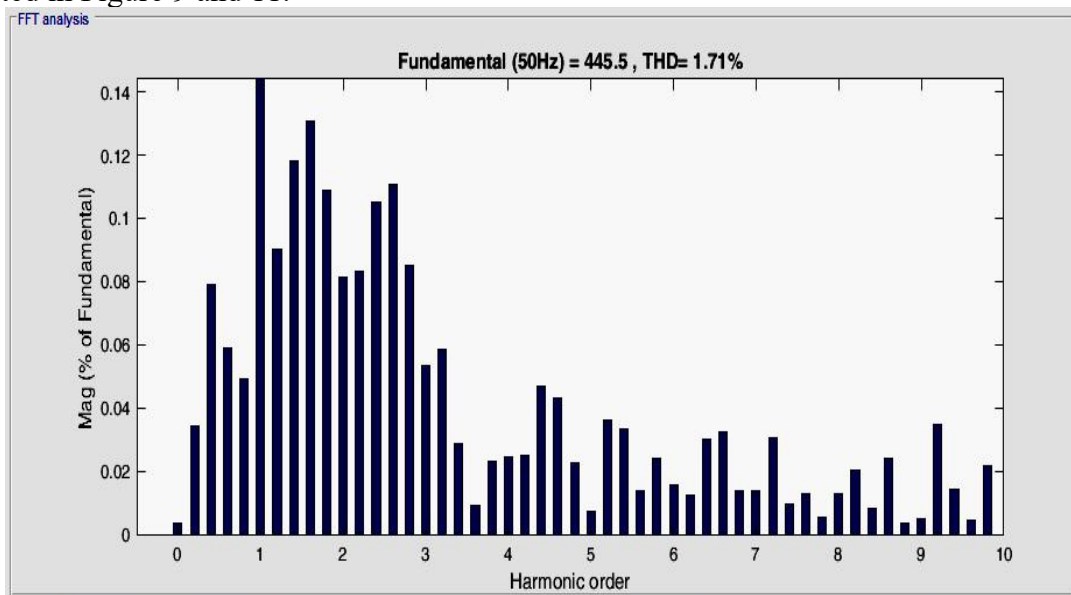


**Figure 13:** Harmonic analysis of Synchronised grid and inverter voltage when GCI is integrated with the αβPLL
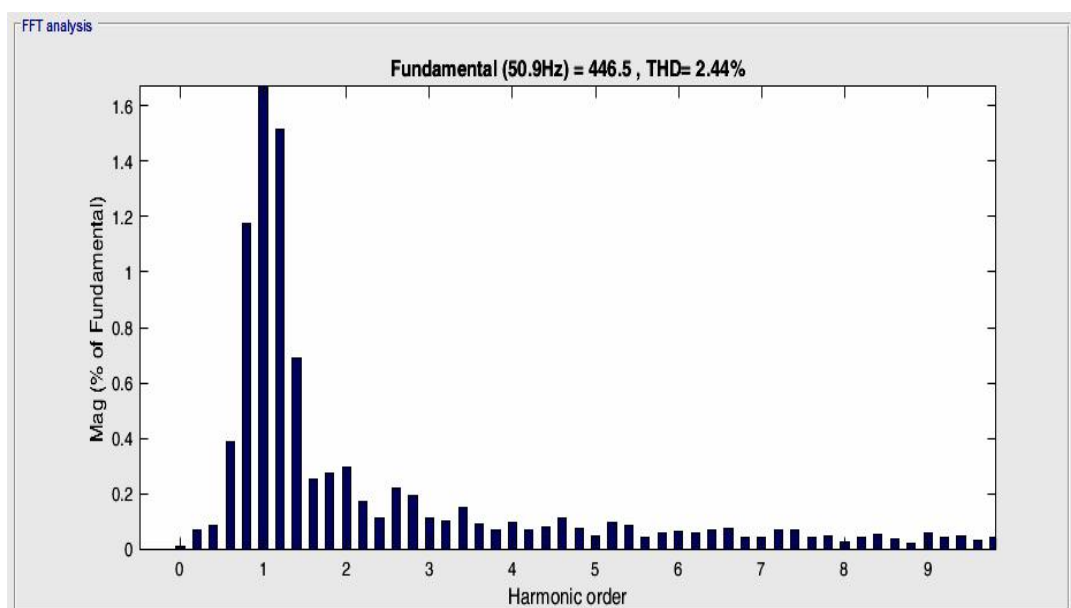


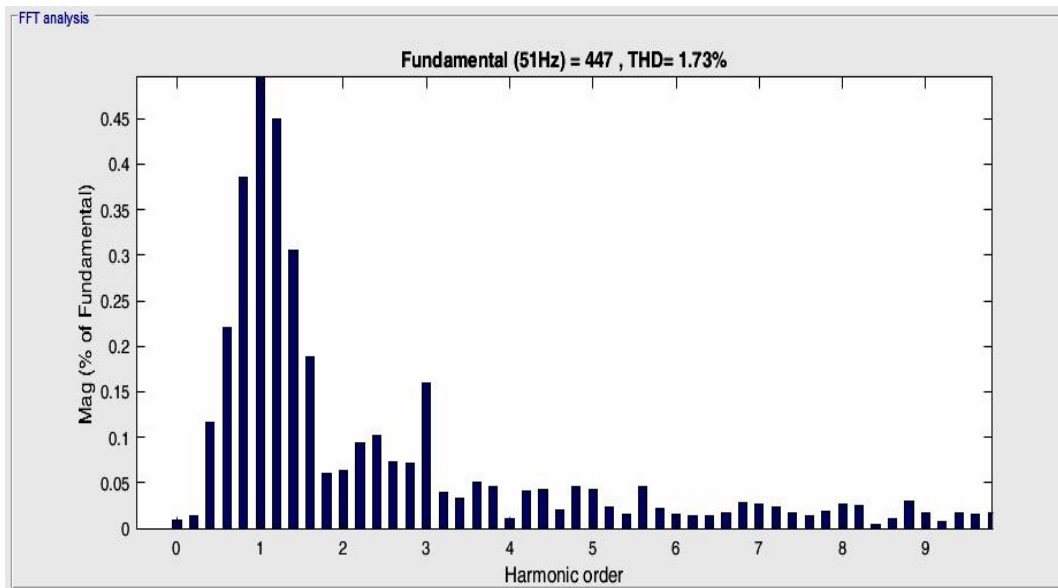**Figure 14:** Harmonic analysis of Synchronised grid and inverter voltage when GCI is integrated with the dqPLL

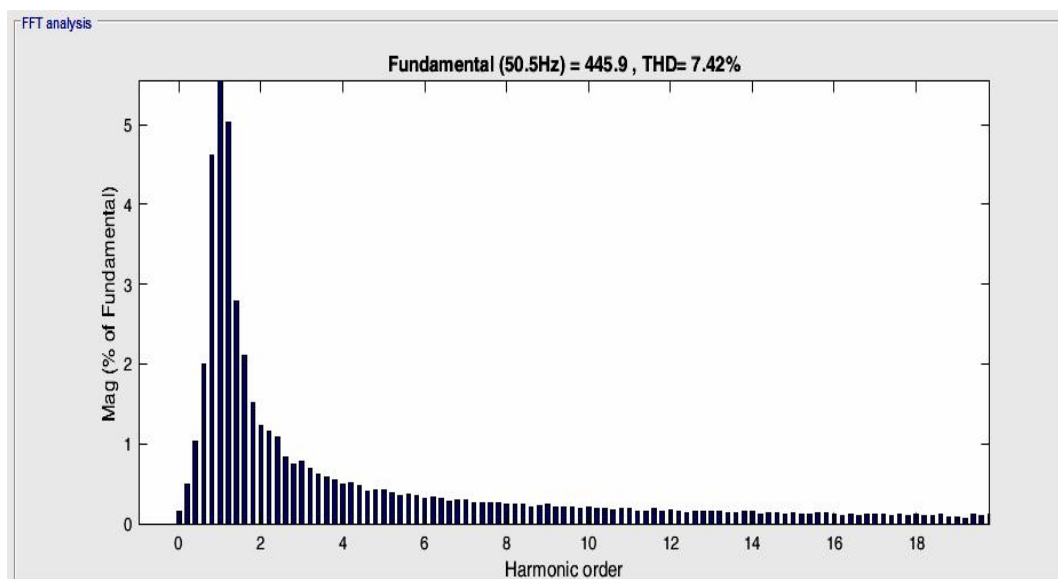**Figure 15:** Harmonic analysis of Synchronised grid and inverter voltage when GCI is integrated with the αβPL*L*



**Figure 16:** Harmonic analysis of Synchronised grid and inverter voltage when GCI is integrated with the dqPLL

It was observed that αβPLL present a good harmonic filtering capability with a THD 1.71% and 1.73% when $2^{nd}$ and $3^{rd}$ order harmonics were subjected to the grid voltage as shown in Figure 13 and 15 respectively. While it was observed that *dq*PLL represent a fair harmonic filtering capability with a THD 2.4% when $2^{nd}$ order harmonics are present in the grid voltage as shown in Figure 14. However, when the grid is distorted with $3^{rd}$ order harmonics, it didn't

show a good harmonic filtering capability with THD of 7.42% as shown in Figure 16.

**Stability analysis of αβPLL and dqPLL algorithm**

Using the transfer function of equation 10 and 11, the poles of the characteristics equation were obtained using stability analysis. The result from the analysis for the stationary αβPLL and dqPLL is shown in Figure 17 and 18. It can be seen that all the pole are located on the left hand side of the s-

plane, this result depict that αβPLL synchronization technique is marginally stable as shown in Figure 17. While it is observed in Figure 18 that some of the pole are located on the right hand side of the s-plane, this result depict that *dq*PLL synchronization technique is unstable.

$$Y_{\alpha\beta}(s) = \frac{-2.229\times10^{10}s^2 - 1.885\times10^{10}s - 1.908\times10^8}{s^5 + 2.516\times10^4 s^4 + 6.561s^3 + 11.08s^2 + 8.731s + 2.911} \qquad (10)$$

$$Y_{dq}(s) = \frac{-1.42\times10^{11}s^2 - 3.409\times10^8}{s^5 + 4.758\times10^4 s^4 + 12.33s^3 + 24.18s^2 + 31.21s + 15.09} \qquad (11)$$



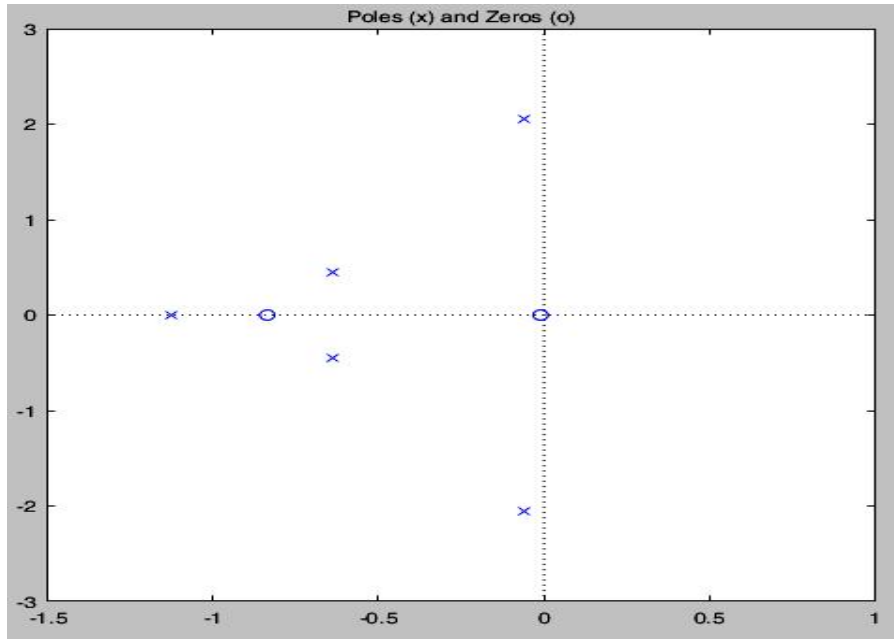**Figure 17:** Poles and zeros from stability analysis of stationary αβ reference phase locked loop (PLL)
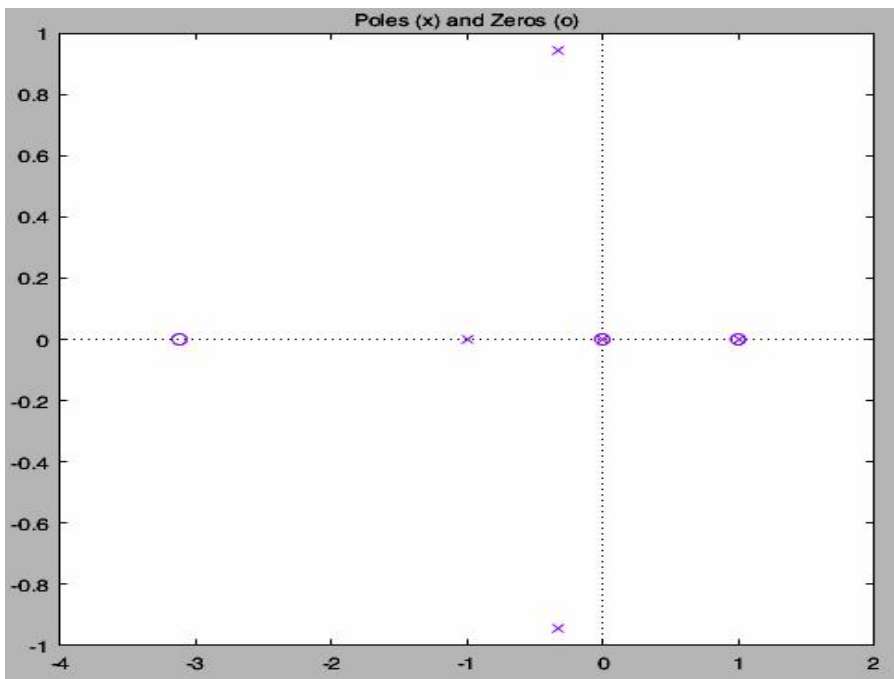


**Figure 18:** Poles and zeros from stability analysis of Synchronous dq reference phase locked loop (PLL)

## CONCLUSION

We found that, the stationary "αβ" reference frame outperform synchronous "dq" reference frame Phase Locked Loop (PLL) synchronization algorithm in term of stability, harmonic filtering capability, frequency shift and phase jump. Our investigation revealed that both the αβPLL and dqPLL, exhibited proficient phase detection capabilities under normal grid conditions. Moreover, when subjected to grid distortions involving phase jump, frequency shift and harmonic distortion, αβPLL perfectly synchronized the inverter with the grid voltage. The disparity in performance between the two techniques is substantiated by a thorough analysis of stability in the PLLs algorithm. It was evident that the αβPLL synchronization technique is well-suited for ensuring successful inverter-grid synchronization, even in the presence of distortion in the grid. The implications of this favourable performance of αβPLL algorithm signifies the potential for seamlessly integrating a substantial amount of power from grid-connected inverters into the utility grid. This, in turn, ensures the injection of an ample power supply for community consumption, contributing to a more robust and reliable energy infrastructure.

## REFERENCES

Akhtar, M. A., & Saha, S. (2020). Analysis and comparative studies on impact of Transport Delay and Transforms on the performance of TD-PLL for single phase GCI under grid disturbances. *International Journal of Electrical Power and Energy Systems*, 105488.

Ali, M. H., Sisa, A. A., & Ahmed, A. B. (2022). An Optimal Control Technique for Single-Phase Grid-Connected Inverter. *Nigerian Journal of Technology (NIJOTECH)*, *41*(3), 578–584.

De la Sen, M. (2007). Stability criteria for linear time-invariant systems with point delays based on one-dimensional Routh-Hurwitz tests. *Applied Mathematics and Computation*, *187*(2), 1199–1207.

Hadjidemetriou, L., Kyriakides, E., Yang, Y., & Blaabjerg, F. (2016). A Synchronization Method for Single-Phase. *IEEE Transactions on Power Electronics*, *31*(3), 2139–2149.

Hadjidemetriou, Lenos, & Yang, Y. (2019). A Synchronization Scheme for Single - Phase Grid - Tied Inverters under Harmonic Distortion and Grid Disturbances. *IEEE TRANSACTIONS ON POWER ELECTRONICS*, *35*(2), 255–266.

IEEE Std 519. (2014). IEEE Std 519-2014 (Revision of IEEE Std 519-1992), IEEE Recommended Practice and Requirements for Harmonic Control in Electric Power Systems. *IEEE Std 519-2014 (Revision of IEEE Std 519-1992)*, *2014*, 1–29. http://ieeexplore.ieee.org/servlet/opac?punumber=6826457

Jaalam, N., Rahim, N. A., Bakar, A. H. A., Tan, C., & Haidar, A. M. A. (2016). A comprehensive review of synchronization methods for grid-connected converters of renewable energy source. *Renewable and Sustainable Energy Reviews*, *59*, 1471–1481.

Meral, M. E., & Celik, D. (2018). *DSOGI-PLL Based Power Control Method to Mitigate Control Errors Under Disturbances of Grid Connected Hybrid Renewable Power Systems*. 81–91.

Rey-boue, A. B. (2017). *Overview and comparative study of two control strategies used in 3-phase grid-connected inverters for renewable systems*. *19*(01).

Sepahvand, H., Saniei, M., Mortazavi, S. S., & Golestan, S. (2021). Performance improvement of single-phase PLLs under adverse grid conditions: An FIR filtering-based approach. *Electric Power Systems Research*, *190*, 106829.

Suleiman, L., Koki, F. S., & Ali, M. H.

(2016). Investigating The Effects Of Irradiance And Temperature On The Performances Of PV Modules Technologies. *International Journal of Innovative Research and Advanced Studies (IJIRAS)*, *3*(7), 196–200.

Wang, Y., Chen, X., Wang, Y., & Gong, C. (2019). Analysis of frequency characteristics of phase-locked loops and effects on stability of three-phase grid-connected inverter. *International Journal of Electrical Power and Energy Systems*, *113*, 652–663.

Xu, J., Qian, Q., Zhang, B., & Xie, S. (2019). Harmonics and Stability Analysis of Single-Phase Grid-Connected Inverters in Distributed Power Generation Systems Considering Phase-Locked Loop Impact. *IEEE Transactions on Sustainable Energy*, *10*(3), 1470–1480.

Youness, E. M., Aziz, D., Abdelaziz, E. G., Jamal, B., Najib, E. O., Othmane, Z., Khalid, M., & Bossoufi, B. (2019). Implementation and validation of backstepping control for PMSG wind turbine using dSPACE controller board. *Energy Reports*, *5*, 807–821.

Yu, J., Yang, B., Zhu, P., Zhang, L., Peng, Y., & Zhou, X. (2022). An improved digital phase locked loop against adverse grid conditions. *Energy Reports*, *8*, 714–723.

Zhang, C., Wang, X., & Blaabjerg, F. (2015). Analysis of phase-locked loop influence on the stability of single-phase grid-connected inverter. *2015 IEEE 6th International Symposium on Power Electronics for Distributed Generation Systems*.